Theoretical and Applied Climatology (2024) 155:3581–3597
https://doi.org/10.1007/s00704-024-04830-z

RESEARCH

Wind energy potential of weather systems affecting South Africa's Eastern Cape Province

Greg Landwehr[1] · Chris Lennard[2] · Francois Engelbrecht[1]

Received: 1 June 2023 / Accepted: 2 January 2024 / Published online: 27 January 2024
© The Author(s) 2024

Abstract

As a percentage of the total global energy supply, wind energy facilities could provide 10% of the total global energy supply by 2050 as reported in IEA World Energy Outlook (2022). Considering this, a just transition to renewable and sustainable energy in South Africa is a genuine possibility if steps are taken immediately to achieve this. The Eastern Cape Province exhibits a strong wind resource which can be exploited towards expediting such a just energy transition. No research and related modelling have, to date, been undertaken in quantifying and relating the detailed P50 energy yield analyses of representative wind energy facilities in temporal and spatial dimensions to the occurrence of specific synoptic types in South Africa. To quantify this energy meteorology climatology for a suitably sized geospatial area in the Eastern Cape Province of South Africa (spatial focus area, latitude −30 to −35, longitude 20 to 30), the approach of using self-organising maps is proposed. These maps are used to identify the most common synoptic circulation types occurring in the Eastern Cape and can subsequently be mapped onto an equivalent time resolution wind energy production timeseries calculated based on probable wind energy facility sites. This paper describes comprehensive methodologies used to model the wind energy facilities, calculate with high confidence the P50 energy production, and then identify the predominant synoptic weather types responsible for the wind energy production in this spatial focus area. After quantifying the energy production, running a self-organising map software generates a purposely selected 35 node map that characterises archetypal synoptic patterns over the 10-year period. The synoptic types can be ranked by the highest energy production. It is shown that in this spatial area, monthly wind energy production is higher during the winter months. When the well-established high-pressure cells move northward, synoptic types associated with higher energy production are frequent and include tropical and temperate disturbances across South Africa, patterns resembling a ridging anticyclone off the west coast of South Africa and low-pressure cells occurring to the north and south. Low energy producing patterns show characteristics of the high-pressure cells moving southwards producing fine weather and mildly disturbed conditions. The purpose of this methodology is that it provides the foundation required to derive long-term frequency changes of these synoptic weather systems using global climate model ensembles and thus changes in wind energy production.

1 Introduction

In South Africa, a seminal paper on renewable energy, written in 2003, recognised that the long-term potential of renewable energy is substantial (Department of Mineral Resources and Energy 2003). Wind energy has also been given priority by the Integrated Resource Plan (IRP) (Department of Mineral Resources and Energy 2019). This positive outlook for renewable energy, in particular wind energy, in South Africa requires long-term strategic planning to realise that potential.

A single wind energy facility (WEF) typically takes 2 to 4 years to build (Department of Mineral Resources and Energy 2022) and integrating such facilities with existing distribution

✉ Greg Landwehr
0701540k@students.wits.ac.za

Chris Lennard
lennard@csag.uct.ac.za

Francois Engelbrecht
francois.Engelbrecht@wits.ac.za

[1] Global Change Institute, University of the Witwatersrand, 1 Jan Smuts Ave, Johannesburg 2000, South Africa

[2] CSAG, University of Cape Town, Rondebosch, Cape Town 7700, South Africa

and transmission networks requires consultation with utilities on tie in solutions whilst always referencing their Generation Connection Capacity Assessment (GCCA) (Eskom Holdings 2022). WEF development is dependent on the strength of the wind resource itself and the process involved requires onsite measurement instruments as well as well-defined statistical techniques to characterise the wind resource. As a rule, banks and other investors demand at least 1 year of measured wind resource data and an independent third-party evaluation from a well-established energy yield consultant before committing investment to a new WEF.

As part of deciding the location of a new WEF, climate variability and change should be considered. Important is optimal energy production over the lifespan of the generators and associated power purchase agreement (PPA), which may well be 20 years or longer. Such planning extends to the reuse of the site after the wind turbine generator (WTG) lifespans are over implying, the need to include climate change assessments beyond the near-term (the next 20 years).

In this study, the Eastern Cape (EC) of South Africa is selected as the area of interest since it has strong potential for WEF development with annual average wind speeds of greater than 7.2 m/s (at 62 m, the local Wind Atlas of South Africa (WASA) mast's highest anemometer) and capacity factors above 40% at the sites investigated in this paper. The province has and is expected to be extremely competitive in the future bid rounds of the Renewable Energy Independent Power Producer Procurement Programme (REIPPPP) and private sector PPAs (Department of Mineral Resources and Energy n.d.).

To characterise the wind potential of the Eastern Cape in more detail, four fictitious WEFs are modelled, each purposefully located close to the WASA (The wind atlas of South Africa n.d.) meteorological masts. These masts provide 10 years of 10-min average wind resource measurements, from 2010 to 2019. This allows for the energy production at P50[1] level to be calculated with high certainty given the 10-year measurement period.

To quantify the energy-meteorology climatology of the Eastern Cape Province of South Africa, a synoptic typing methodology is used to objectively identify the main synoptic weather systems that provide wind potential to the province. Characterising these synoptic types and the resultant energy production associated with each can inform WEF siting for both the current climate and future climate that may change due to global warming.

This paper begins by presenting the background information in Section 2 which is necessary to generate the results. Methodologies used in the study are presented in detail in Section 3 and the results and discussion follow in Section 4, with conclusions drawn in Section 5.

2 Background

2.1 South African electricity supply system

South Africa exhibits one of the most carbon-intensive electricity supply systems in the world and is currently striving towards a 'Just Energy Transition' which is less carbon-intensive (European Commission 2022). South Africa's power Generation, Transmission and Distribution systems are dominated by Eskom.[2] The parastatal generates 90% of South Africa's electricity with a current power plant capacity for South African consumption of approximately 46.5 Gigawatts (GW) most of which comes from coal (Eskom Holdings n.d.). This varies at any one time due to electricity trading with neighbouring countries and issues such as load shedding and unforeseen plant maintenance. As per the latest South African census, the electrification ratio in South Africa is at 87% (South African census 2011).

During the last decade, South Africa has developed approximately 6 GW of combined wind, solar photovoltaic (PV), and concentrated solar power (CSP) (CSIR Energy Centre Analysis 2020). Projections made by the Department of Mineral Resources and Energy show that the electricity generation capacity of South Africa could rise to 109 GW by 2050 with 33% (capacity and electricity production) coming from wind alone (Department of Mineral Resources and Energy 2019). If such a change materialises, it will have extensive benefits beyond energy generation and would contribute to South Africa's emissions reduction efforts.

2.2 WEF siting

Of course, WEF siting can follow different methodologies; however, the following description provides a general overview of the major steps that any WEF siting exercise will employ. Initially, mesoscale average annual wind speed and power density[3] maps are used to select pre-feasibility positions for WEFs. Once a pre-feasibility position is selected, it is scrutinised against a set of pre-feasibility criteria such as proximity to the electrical grid, avifaunal/faunal no-go

[1] P50 energy yield: the net annual energy production (AEP) value is considered the 'P50' energy yield value and constitutes the gross AEP value less losses that has the probability of being exceeded by 50% of all AEP's that could be possible for the site involving the uncertainties associated with the estimate.

[2] Eskom: Eskom Holding SOC. Ltd. is South Africa's primary electricity supply utility.

[3] Power density: mean annual power available per square metre of rotor blade swept area of a suitable WTG.

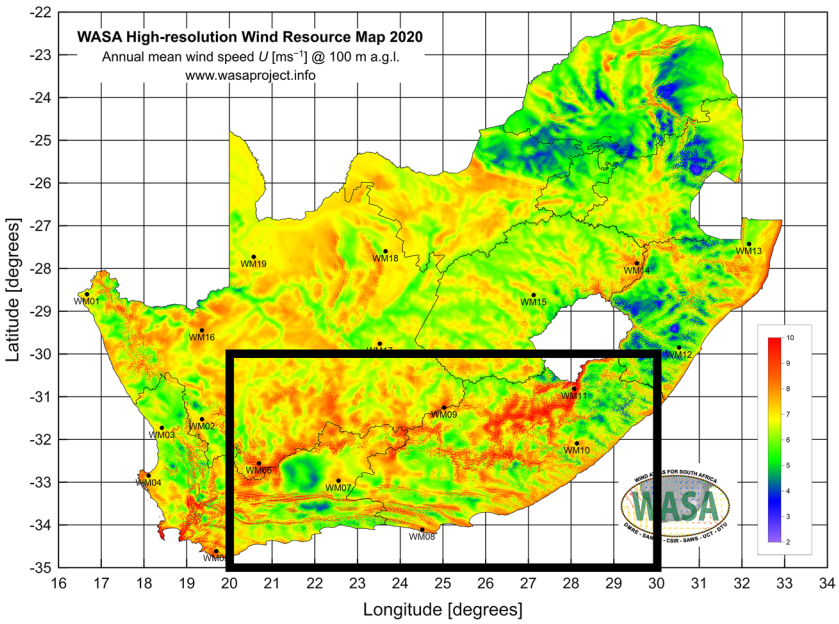

Fig. 1 The geographic location of the study region within South Africa using the WASA wind speed map (colour bar shows annual average wind speed in m/s) (The wind atlas of South Africa n.d.)

areas, protected flora areas, proximity to existing buildings and infrastructure, and road access.

Once the site passes this screening, feasible wind turbine layouts are created based on wind flow maps which are created using the onsite measurement data. The WEF layout design is undertaken using specialised WEF modelling software (sometimes requiring computational fluid dynamic analysis for complex terrain) which considers terrain, roughness, and wake losses. Then, high level net capacity factor (NCF[4]) and AEP[5] calculations are completed to verify the attractiveness of the site. These calculations are based on at least 1 year of observed measurements from the site.

2.3 Geospatial area of interest

The Eastern Cape Province of South Africa (Fig. 1) has a strong potential for wind energy. The WASA map (The wind atlas of South Africa n.d.) shows a significant part of the Eastern Cape Province having annual average wind speeds in the order of 7–8 m/s and accompanied by wind power densities in the order of 300–600 W/m^2. This makes the Eastern Cape a viable location for utility scale wind farms. As a reference dataset for selection of the spatial area of interest, WASA is an important reference. Similar Wind Atlases have been developed to provide comparable insights globally (Hahmann et al. 2020; Nassar et al. 2023).

Accompanying these high annual average wind speeds are very attractive NCFs which can range between 35 and 45% for the Eastern Cape and have been extremely competitive in the past bid rounds of the REIPPPP (Department of Mineral Resources and Energy n.d.). In contrast to this, similar quality sites (Global Wind Atlas, 2023) with high density of WEFs installed exist in North Brazil (~45% NCF), the Egyptian coast of the Gulf of Suez (~50% NCF), Northern Germany (~40%), and South India (~40%).

Four fictitious WEF sites (Fig. 2) have been selected to adequately cover the selected area of interest and have been chosen due to their proximity to four WASA masts. Furthermore, they are named after the WASA masts from which the energy production timeseries is derived, WM07 (−32.967°, 22.556°), WM08 (−34.110°, 24.514°), WM09 (−31.252°, 25.031°), and WM10 (−32.092°, 28.136°) and are located between 5 and 10 km from their namesake WASA mast to the outermost WTGs. Energy production at P50 level can thus be calculated with high confidence since it is based on 10 years of high-resolution wind resource measurements from 2010 to 2019 taken from the WASA.

The general WEF and WTG specifications used for the modelling are provided in (Table 1):

2.4 Synoptic-scale weather systems impacting on the Eastern Cape

Located in Southern Africa, south of 30 °S, the climatology of the Eastern Cape is determined by a range of different weather systems that originate in climatological circulation

[4] Net capacity factor: the actual annual net energy yield / theoretically possible annual energy yield if the plant ran at full capacity all year around. *NCF = Actual Energy Generated less all losses (MWh) / (Plant Capacity (MW) × Time Period (h))*

[5] Annual energy production: actual annual gross energy production less losses

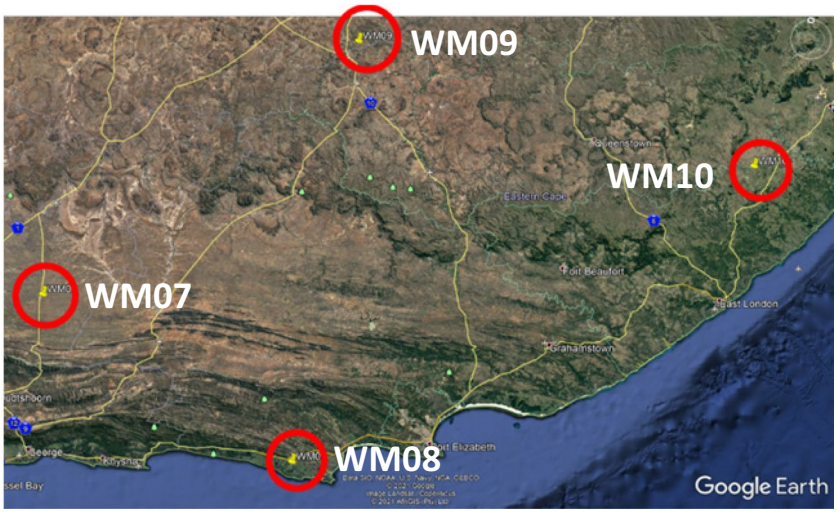

Fig. 2 WEF geographical positions within the geospatial focus area

Table 1 WEF general specifications

WEF capacity (MW)	Between 148.5 and 192.5
Wind turbine generator type and nameplate capacity	3-bladed, horizontal axis, 5.5 MW
Hub height (m)	120
WTG rotor diameter (m)	155
Number of WTGs	Between 27 and 35
Assumed voltage connection level (kV)	132

zones including Southern Hemisphere westerlies, the Southern Hemisphere subtropics, and the African tropics. The coastal areas of the province are in fact a year-round rainfall zone (Engelbrecht et al. 2015), where cold fronts from the westerlies in winter alternate with thunderstorm producing weather systems in summer to bring all-year rainfall.

The most important synoptic-scale weather systems determining the provinces' climatology, in terms of both rainfall and wind, are mid-latitude cyclones, ridging high-pressure systems, cut-off lows, and tropical temperature troughs. These weather systems introduce some meso-scale circulation patterns such as Berg winds, which are also important in terms of the wind climatology.

2.4.1 Mid-latitude cyclones and cold fronts

Key to Eastern Cape's wind climatology is the frequent passage of mid-latitude cyclones in the Southern Ocean to the south, the cold fronts embedded within these systems, when occurring at sufficiently northerly latitudes, bring distinct wind patterns to the Eastern Cape. Ahead of an approaching cold front, winds are dry and from the northwest, whilst cool or cold high southwesterly winds blow behind the front. These frontal systems are positioned more Equatorward in winter and occur more frequently and intensely during these months. They can on occasion penetrate deep into the southern African interior during 'cold snap' events, and substantially increase the energy demand in order to achieve human comfort (Tyson and Preston-Whyte 1988).

2.4.2 Ridging anticyclones

The South-Atlantic Ocean High typically ridges in behind cold fronts affecting the Cape south coast regions of South Africa, including the Cape south coast (Ndarana et al. 2020). The ridging process initially strengthens the southwesterly flow behind the cold front, but as the process continues, the flow can become pronounced southeasterly. Such ridging high-pressure systems are consequently important sources of not only wind energy for the Eastern Cape, but also of moisture and rainfall (Engelbrecht et al. 2014). Rainfall can be particularly heavy if the system co-occurs with a cut-off low (Engelbrecht et al. 2014).

2.4.3 Upper-air troughs and cut-off lows

All mid-latitude cyclones are three-dimensional weather systems, with upper air troughs typically occurring to the west of the surface cold front, and with rainfall occurring to the east of the upper air trough. When an upper air trough becomes separated or 'cut-off' from the westerly wind regime, it is referred to as a 'cut-off low'. The generally slow-moving cut-off lows are responsible for many of the flood producing rains in South Africa, including the Eastern Cape (Engelbrecht et al. 2013; Engelbrecht et al. 2015). Their frequency peaks in March to May and September to November with lower frequency between December and February (IEA 2022). Cut-off lows and upper-air troughs frequently cause several days of cloud cover, implying their indirect importance to the wind-energy sector (i.e. via

reduced solar potential). Moreover, cut-off lows are associated with pronounced southeasterly flow over the Eastern Cape (Engelbrecht et al. 2015).

2.4.4 Coastal low and Berg wind

Several meso-scale weather systems and phenomena induced by the synoptic-scale flow also impact on Eastern Cape climatology. Coastal lows form in the northwesterly flow ahead of an approaching cold front due to the generation of cyclonic vorticity when air descends from the South African plateau. They are associated with strong meso-scale pressure gradients with northwesterly flow to the east, and southwesterly flows to the southwest of the centres of these systems (Tyson and Preston-Whyte 1988).

A further mesoscale phenomenon associated with the coastal low and approaching cold front, typically occurring in winter, is the 'Berg winds' that form when northwesterly winds descend over the southern escarpment and warm adiabatically to produce high surface temperatures over the Eastern Cape. These Fohn-type winds (Tyson and Preston-Whyte 1988; Tyson 1964) occur most commonly in winter due to the relatively high frequency of passing frontal systems during this season.

2.4.5 Temperate disturbances in the westerlies

Fine-weather and mildly disturbed conditions over the Southern African interior occur in association with large subtropical high-pressure systems centred over the subcontinent. These systems produced fine clear conditions and little or no rainfall, and impact on the northern interior regions of the Eastern Cape. The frequency of occurrence of anticyclones reaches a maximum over the interior plateau in June and July with a minimum during December.

2.5 Wind farm modelling software

Two different tools, WAsP © and OpenWind ©, have been utilised to calculate the energy production at each WEF site to provide further robustness to the results. Both are industry leading tools used for wind data analysis, wind atlas creation, wind farm energy yield analysis, and siting of WTGs. Note that steps 3 and 4 in Section 3.1 can be undertaken automatically in Openwind © if input loss and uncertainty values are setup within the software.

2.5.1 WAsP ©

As per the methodology outlined in preceding sections, the linear downscaling software WAsP © has been used in a semi-manual approach to generate AEP for each site. The spatial and temporal distribution of the wind resource is provided in the form of a wind resource grid (WRG) and uses a virtual WTG. The AEP results are then post-processed using bespoke built spreadsheet calculators (Danish Technical University n.d.-a).

The wake loss model used is Modified Park (Park 2) using a wake decay constant of 0.09 (Danish Technical University n.d.-a).

2.5.2 OpenWind ©

Calculating the expected energy production of wind turbines in an array is the basic function of Openwind © which follows in principle the same steps outlined in steps 3 to 4 of Section 3.1 and uses a mass consistent approach. The spatial and temporal distribution of the wind resource is also provided in the form of a wind resource grid and the characteristics of the WTGs with loss assumptions complete the main input elements for the calculation (Underwriter Labs n.d.).

Although there are many options, the wake loss model used is also Modified Park to remain consistent with WAsP © and uses a wake decay constant of 0.09 (Underwriter Labs n.d.).

2.5.3 Validation of the WEF modelling software

To verify that the equations and assumptions used in the OpenWind © energy production calculations, AWS Truepower has carried out a comprehensive validation exercise involving 20 real-world wind projects, using as a control the WindFarmer program of Garrad Hassan and Partners, Ltd. (Underwriter Labs (UL) 2010). A comparison of the energy production results is supplied in Section 4.2 for both WAsP © and Openwind © at the sites chosen to provide confidence that similar results are obtained from the different software.

2.6 Self-organising maps (SOMs)

To quantify the energy-meteorology climatology of the Eastern Cape Province, the approach of using SOMs is proposed. These maps are used to objectively identify the prevailing synoptic weather types occurring in the Eastern Cape Province of South Africa.

The field of climatology has widely adopted the use of SOMs, a machine learning-based approach to clustering, in recent years and was introduced to the field in 2002 (Doan et al. 2020). Kohonen originally developed SOMs (Kohonen et al. 1996) for data mining. SOMs discover patterns intrinsic to complicated input datasets and as a result can generate a cluster of simplified representations of the dataset, called nodes. The most important patterns of the input dataset are represented by the nodes (Doan et al. 2020). Synoptic weather typing is an original use of applying SOMs in climatology (Sheridan and Lee 2011) as used in several studies

over South and Southern Africa (Lennard and Hegerl 2014; Pinto et al. 2015) and elsewhere (Hewitson and Crane 2002; Hope 2006; Sammon 1969).

The algorithm used by a SOM iterates and gradually updates the makeup of the nodes in the data space until it results in a converged solution, i.e. the 'best' summarised representation of the input data. For each iteration, the algorithm chooses a random input vector and matches it to one of the nodes. The 'winning' node is called the best matching unit (BMU) (Doan et al. 2020).

Training is then carried out by adjusting the BMU and its neighbours to become closer to the input vector. The learning rate and neighbourhood function are key inputs that govern the training task. Traditional SOMs use the Euclidean distance (ED) to search for the BMU, where the 'closest' node to an input vector in terms of ED will be assigned as the BMU (Doan et al. 2020).

2.6.1 SOM software

The SOMPAK © software package (Kohonen et al. 1996) is one of the earliest realisations of the SOM methodology. It contains all programs necessary for the correct application of the SOM algorithm to visualise and cluster the ERA5 geopotential dataset.

2.6.2 SOM input dataset

For the purposes of this study, the fifth generation of the European Centre for Medium-Range Weather Forecast's Atmospheric Reanalysis dataset (ERA5) (Hersbach et al. 2020; European Centre for Medium-Range Weather Forecasts, ERA5 n.d.) at six hourly and ~0.28° (TL639[6]) temporal and spatial resolution respectively has been used for the period 2010 to 2019 to correlate with the equivalent resolution wind resource and energy production data. ERA5 geopotential at 1000 hPa, converted to geopotential height by dividing with 9.81 m/s^2, is used as the variable to characterise the 6-hourly circulation patterns.

The data covers the Earth on a ~ 30-km grid and resolves the atmosphere using 137 levels from the surface up to a height of 80 km. ERA5 data is known to provide a realistic representation of African rainfall patterns (Engelbrecht and Steinkopf 2022) and likely also of the underpinning circulation patterns.

[6] Spectral coefficients or Gaussian grids are the method in which ERA5 data is archived to provide a somewhat uniform spacing over the globe. The ERA5 high-resolution (HRES) wind resource data are archived on a reduced Gaussian linear grid and in the case of this study, the name of the grid is TL639 (European Centre for Medium-Range Weather Forecasts, ERA5 n.d.).

The domain for which the geopotential dataset was extracted spans Southern Africa (16°E to 34°E and 22°S to 35°S), with the relevant smaller Eastern Cape domain of interest contained within the larger domain. To provide a normalised input for the SOM software, so that the seasonal differences in geopotential height do not dominate the SOM-derived synoptic types, the spatial average of geopotential across the Eastern Cape domain was subtracted from the value at each ERA5 grid point. That is, the SOM is developed using the special anomalies of geopotential, following Engelbrecht et al. (2015).

3 Methodology

The proposed methodology that follows is carried out in three major steps namely:

1. Energy yield analysis:

- Step 1: Meteorological data acquisition and wind resource analysis
- Step 2: WEF modelling
- Step 3: Net AEP energy yield analysis
- Step 4: Daily energy production calculation

2. SOM training
3. Energy mapping:

- Step 1: Match energy production to each node
- Step 2: Identifying the corresponding synoptic type for each of the 35 SOM nodes

3.1 Energy yield analysis

A crucial part of the energy yield analysis for a WEF is a sufficiently long period of observed wind resource time-series, derived from measurement instruments mounted on a meteorological mast on the site. This observed wind resource data generally needs to be properly quality controlled to make sure there are no anomalies that could impact the energy production calculations.

Step 1: Meteorological data acquisition and wind resource analysis:

The typical process, also applied here, is recommended as follows:

1. Confirmation that the duration of measurement is longer than 1 year. In this case, 10 years of measured data was available to use from the WASA meteorological masts.

Note that the requirement of having data for at least 1 year is currently a general requirement of lenders and from a climatological perspective, a period of at least 20 years would have been preferred to fully characterise the inter-annual variability of weather systems.

2. Perform a visual inspection of the dataset to identify missing portions of data and remove severe outliers.
3. Make sure data availability is greater than 99% for the highest anemometers for the duration of the measurement period. If this is not achievable, then other available anemometers can be used for data filling.
4. Verify all timestamps to make sure they are consecutive.
5. Data quality control:

a. Remove data that is greater than 18 days corrupted.
b. Replace data that is corrupted for less than 18 days and greater than 1 day from alternate instruments on the meteorological mast.
c. Repair values corrupted for less than 1 day by using data from a previous or subsequent day or take averages of the previous and following several days or fill data/extrapolate from another anemometer.
d. Perform a plausible value check to make sure the measured values are within reasonable limits.
e. Perform a plausible rate of change check to make sure that there are no unreasonable step changes in the data.
f. Perform a tower shadow analysis to adjust measurements affected by the meteorological masts tower shadow.
g. Perform a long-term adjustment using the closest node from a long-term reanalysis dataset such as ERA5 or MERRA2.

Similar methodologies have been employed by studies carried out globally and reinforce the use of reanalysis datasets for not only long-term correction but, where there is no measurement data, these datasets can be used as the base dataset in the quantification of the wind energy production, each of course having their unique strengths as outlined by Gruber et al (Gruber et al. 2022). Some examples of such Wind Resource Assessment methodologies can be found from Oman and Thailand in (Khan et al. 2023) and (Charabi et al. 2019).

Step 2: WEF modelling:

The fundamental components that constitute the wind farm model are outlined below, followed by the calculation procedures:

a. An underlying digital terrain model (DTM[7]).
b. A preferred wind farm layout adhering to standard 3 rotor diameter (non-predominant wind direction) × 9 rotor diameter (predominant wind direction) WTG spacing to minimise internal WEF wake losses.[8]
c. A suitable virtual WTG model based on the original equipment manufacturer's (OEM's) power curve for the correct turbulence intensity, wind class, and air density at the WTG's hub height.
d. A virtual meteorological mast which is a virtual representation of the data derived from step 1.
e. A wind resource grid (WRG) is derived from the Wind Atlas Analysis and Application Program (WAsP) method of extrapolation (Danish Technical University n.d.-b) of the actual wind speeds at the met mast position to the actual WTG positions (Danish Technical University n.d.-a). The method of calculating the wind speeds at WTG hub height in the WAsP method makes use of a logarithmic wind profile[9] dictated by the terrain surface roughness (Danish Technical University n.d.-a).

1. Once these items are in place, the wind farm modelling software, in some cases making use of computational fluid dynamics (CFD) in extremely complex terrain, can build the wind flow model and calculate the AEP specific to the wind farm layout, WTG, DTM, and observed wind resource data.
2. This AEP value is typically a gross value with no losses deducted and is based on a typical meteorological year (TMY) derived from the measurements and extrapolated to the WTG positions.

Step 3: Net AEP energy yield analysis:

Considering a normal distribution, the P50 energy production is the centre value and is calculated as follows:

1. The wind energy modelling software calculates the wake losses for each WTG in a WEF and thereby the part-net annual energy production of each WTG turbine, and aggregates this for the entire WEF (The Danish Technical University n.d.-b).
2. Once the gross AEP and the wake loss percentage are known, additional losses can be considered and factored into the final net AEP. These are namely the 'Balance

[7] The digital terrain model associated with the wind farms modelled in this research contains an elevation layer derived from SRTM V.2 publicly available data, with 10-m contour height.

[8] WEF wake losses: disturbance of the free wind speed by the WTG blades, in turn affecting the downstream wind turbines whereby the free wind speed loses some of its energy.

[9] A logarithmic wind profile allows extrapolation of wind speeds measured at a particular height to the hub height of the WTG. The formula used is $U(z) = (u_*/\kappa)\ \ln(z/z_0)$ where z is height from surface, z_0 is the roughness length, u^* is the friction velocity, and K is the Von Karman constant.

of Plant' (BOP) losses and are estimated based on experience and industry accepted norms, calculated where possible and taken from contractual turbine supply agreements. They are made up of the following items:

a. WTG availability (typically ~3%)
b. Electrical efficiency (typically ~2%)
c. WTG performance (typically ~3%)
d. Environmental (typically ~1%)
e. Curtailments (typically ~1%)

3. By applying all loss factors to the gross AEP value, the net AEP can be calculated.
4. Uncertainty: It should be noted that all the steps in such a methodology have inherent uncertainty particularly in the wind resource assessment and energy yield analysis. This can be calculated to determine probability values outside the P50, typically the P75 for lenders; however, since we are concerned only with the P50 in this study, it is not within the scope. As an indication however, the overall standard deviation of the uncertainty associated with the sites covered in this study could range from 8 to 13%.

Step 4: hourly energy production calculation:

1. The final step in the energy production process is to develop an '8760' energy production which is the annual energy at hourly resolution based on the average hourly wind speed for the wind farm for the 10-year period of interest (Frew et al. 2017).
2. Each hourly wind speed for the complete measured timeseries is passed through the WTG power curve to provide an energy production for each hour.
3. This is summed up for one year and compared to the Net AEP derived in step 3.
4. The average hourly windspeed values are then scaled to provide a matching Net AEP to that derived in step 3 thus intrinsically considering all the losses in the hourly average windspeed. This ensures that the WEF will still operate at or close to rated power for suitably high windspeeds.
5. The hourly energy production can then be adjusted to whatever resolution is required to correlate with the reanalysis data weather patterns, for example 6-hourly data from ERA5.

3.2 SOM training

Based on the work done by Engelbrecht et al. (Engelbrecht et al. 2014), who related Eastern Cape rainfall patterns to synoptic types using SOMS, it was decided to use 35 nodes (representing 35 characteristic synoptic type circulation patterns), derived from the ERA5 reanalysis dataset. The SOM was developed over the smaller Eastern Cape spatial area of interest (box in Fig. 1).

SOMPAK © was used to produce the final trained SOM for this study using the following steps:

1 Data preparation: SOMPAK © requires the data for input to be in a matrix $1 \times N$ format prior to execution of the algorithm. To do this, a python script was used to reshape the 2-D ERA5 dataset into a 1-D matrix for input into the SOMPAK © software.
2 Running the SOMPAK © software: SOMPAK © creates the data files of common synoptic type patterns needed for producing the trained SOM map. Once the SOM has been trained using a vector quantisation algorithm (Kohonen et al. 1996), i.e. the SOM with the 35 archetypical synoptic states is produced, it assigns a BMU for each timestep in the input dataset. The specifications used to run the software are as follows:

- Lattice type: rectangular
- Number of iterations: 100,000
- Training: is done in two phases (1) the ordering phase during which the reference vectors of the map units are ordered; (2) the values of the reference vectors are fine-tuned.
- Initial neighbourhood radius: 3 (decreases to 1 during training)
- Initial learning rate parameter: 0.1 (decreases to 0 during training)

3 It is necessary to confirm that the SOM result makes sense by checking the Sammon maps, a 2-D representation of the *n*-dimensional data space (Kohonen et al. 1996). If there are folds in the map, it is difficult to interpret implying that the radius of influence variable needs to be increased.

3.3 Energy mapping

Following the process of characterising the 35 synoptic types, the resultant energy production associated for each can be quantified via an energy mapping process as follows:

Step 1: Match energy production to each node:

Table 2 Annual site wind resource characteristics at met mast height

	WM07 WEF (62 m)	WM08 WEF (62 m)	WM09 WEF (62 m)	WM10 WEF (62 m)
Annual mean wind speed-U (m/s)	6.95	7.22	8.00	6.65
Wind shear exponent (α)	0.163	0.160	0.136	0.137
Weibull k parameter	2.37	2.05	2.34	2.02
Turbulence intensity	0.12	0.12	0.11	0.12
Power density @ 50 m (W/m^2)	268	388	392	278

1. SOMPAK © makes use of Euclidean distance to determine the BMU for each timestamp in the 10-year ERA5 dataset. In this way, each timestep is mapped to a node.
2. It is then possible to map the energy produced in each correlated time step (sum of energy over the 6-h period) to the corresponding SOM node or BMU.
3. The corresponding energy production per timestep is then used to determine the best performing SOM node in terms of energy production.

Step 2: Identifying the corresponding synoptic type for each of the 35 SOM nodes:

1. The Eastern Cape Domain is too small to identify large scale drivers of the regional climate, so the timestamps associated with each node are used to extract the equivalent ERA5 geopotential (spatially normalised) timestamps for a larger spatial area including all South Africa.
2. This was then averaged per SOM node for the whole of South Africa to produce a single representative image of the synoptic type.
3. These can then be compared to commonly occurring synoptic weather types and assigned to the one that matches it the best.

4 Results and discussion

4.1 Wind resource

In summary, each of the four WEF sites has a capacity between 148.5 and 192.5 MW and employ 3-Bladed, 155-m diameter, horizontal axis, 5.5 MW WTGs at 120-m hub height.

Table 2 provides the mean wind speeds of the four wind farm sites amongst other characteristics. The mean wind speeds are typical of a class III wind site as per the IEC wind classification. This implies a good wind resource and power density.

WEF WM09, situated in the North of the EC Province, sees the highest average annual wind speeds with the other three WEFs—WM07 (Eastern EC), WM08 (Southern EC), WM10 (Western EC)—also showing similar profiles. Wind shears tend to be quite different per site with WM07 showing the highest wind shear, i.e. the increase in wind speed with increased height. Finally, the wind speed frequency distribution's k parameter shows WM09 and WM07 have values close to 3 implying relatively stable wind speeds whereas the other two show moderately stable wind speeds. This is corroborated by the relatively low turbulence intensity values (Table 2).

Table 3 summarises the general annual, seasonal, and diurnal site characteristics for each modelled WEF's meteorological mast data. At all four of the sites, the annual average wind speeds, which vary between 7 and 8 m/s, confirm the favourable wind potential that exists across the Eastern Cape. At three of the four sites, most months exhibit the strongest winds around midday. This is likely the consequence of the land-sea temperature gradient being at its strongest around midday, which contributes to enhanced pressure-gradients and high wind speeds. The exception is site WM07, where most months exhibit the strongest wind speeds at night.

At sites WM09 and WM10, average monthly wind speeds peak in winter and remain relatively high in summer. Closer to the coast at site WM08, wind speeds peak in spring and summer but remain relatively high in autumn and winter. At site WM07 over the western interior, autumn and spring are seasons with high wind speeds at night, but with winter recording high values on the average right through the diurnal cycle.

The wind roses (Fig. 3) indicating the predominant wind direction at the near-coastal site (WM08) and western interior site (WM07) predominantly swing between easterlies and westerlies. At site WM09 over the northern interior, wind direction predominantly swings between north westerlies and south easterlies. At site WM10 over the north-eastern interior, there is a more uniform distribution of wind directions, with slightly higher frequencies from the northeast.

Table 3 12 × 24—monthly and diurnal site wind resource characteristics

WM07 WEF

WM08 WEF

WM09 WEF

WM10 WEF

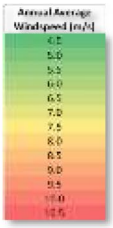

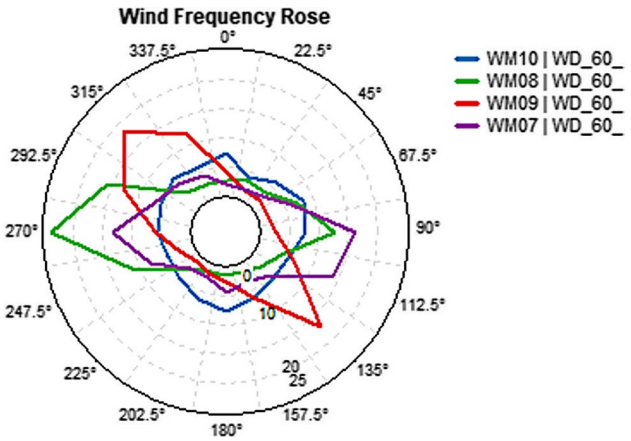

Fig. 3 Wind roses showing predominant wind direction for all Eastern Cape WEF sites

4.2 Energy yield assessment

The P50 annual energy production (AEP) per site is consistent with the wind resource assessment results provided (Table 2). WM09 (41.5% and 42.1%) and WM08 (41.6% and 42.0%) are providing the highest energy production figures and net capacity factors (NCF's) from WAsP © and Openwind © respectively (Fig. 4). WM10 (37.2% and 37.4%) and WM07 (41.8% and 41.3%) WEF sites produce somewhat less energy. In general, the WAsP © and Openwind © versions of the models are producing energy production results that are very similar and differ by no more than 1.5%.

The P50 monthly energy production per site (Fig. 5) shows WM09 providing the highest energy production across the four sites, particularly so in the winter months. The WEF sites generally show higher production in the winter months at WM07, WM09, and WM10. At site WM08, the near coast location, the highest production is simulated for spring.

4.3 SOM results

Following Engelbrecht et al. (2015), a 35 node SOM has been developed to characterise the low-level synoptic circulation types of the Eastern Cape domain (Fig. 6) using 1000-hPa geopotential height anomalies.

To obtain a more extensive spatial view of these systems, the same BMUs used to construct Fig. 6 were applied to construct the relevant circulation patterns over a larger spatial domain (Fig. 7), to obtain better insight into the spatial characteristics, and better identify the synoptic type associated for each of the SOM nodes shown in Fig. 6.

The top-left corner-node of the SOM (node 29, Fig. 6) shows negative geopotential anomalies to the south of the Eastern Cape, and over the southern part of the Eastern Cape, with positive anomalies over the northern interior. This pattern is due to a mid-latitude cyclone approaching from the west (Fig. 7). The bottom-right corner of

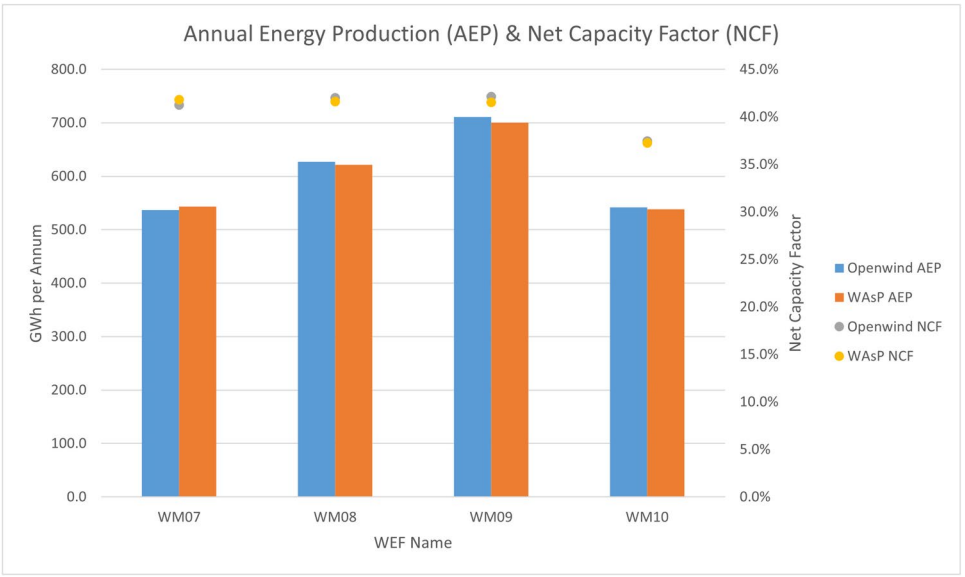

Fig. 4 P50 annual net energy production and net capacity factor per WEF from Openwind © and WAsP ©

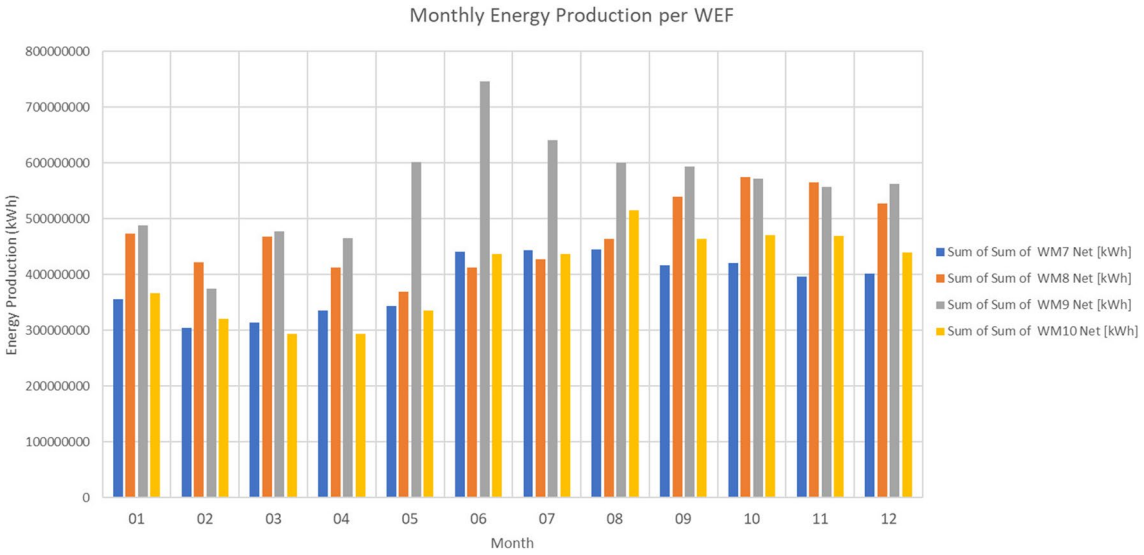

Fig. 5 P50 monthly energy production per modelled WEF site

the SOM (node 7, Fig. 6) shows the 'opposite pattern', positive geopotential anomalies south of and over the southern Eastern Cape, with negative anomalies over the northern interior. This pattern is the consequence of the Atlantic Ocean High starting to ridge along the Cape south coast (Fig. 7). The bottom-left corner of the SOM (node 1, Fig. 6) shows positive geopotential anomalies over the western part of the domain, with negative anomalies to the east. This is due to the Atlantic Ocean High ridging behind a steep trough and cold front (Fig. 7). The 'opposite' pattern appears in the top-right corner of the SOM (node 35, Fig. 6). It is the result of the Atlantic Ocean High ridging further to the east over the South African east coast, with a deep surface trough present over the western interior regions of South Africa.

Because each 6-hourly circulation pattern occurring in the 10-year period is associated with one of the SOM nodes, the energy production of that 6-h period can be mapped onto the relevant node for each of the WEF sites. In this way, it is possible to calculate the energy production associated with each node (Figs. 8 and 9), When ranking the energy production across nodes using Figs. 8 and 9, SOM nodes 8, 15, and 1 (red outline, Figs. 6, 7, and 8) show the largest potential for energy production. All three of these nodes are characteristic of various stages of a deep mid-latitude cyclone passing to the south of the Eastern Cape, with the Atlantic Ocean High ridging behind the cold front over the Eastern Cape.

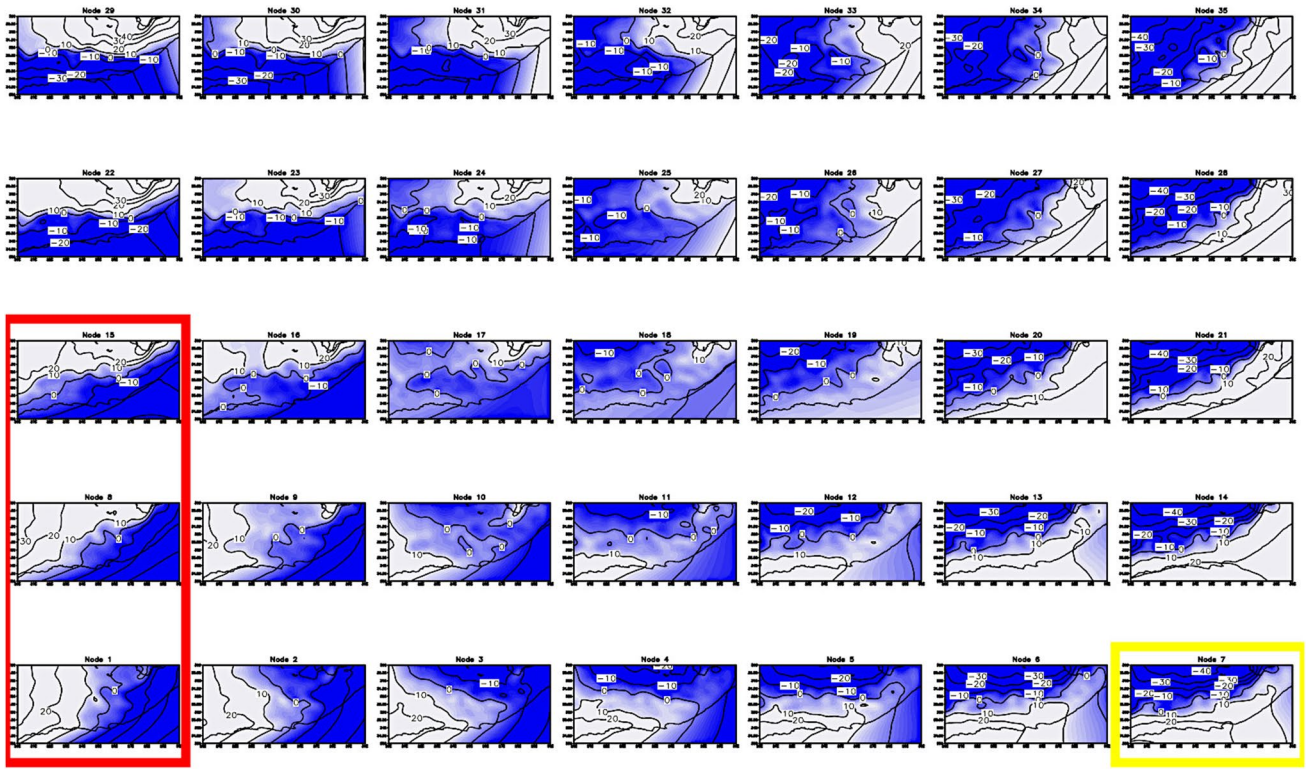

Fig. 6 35-node SOM for geopotential height anomalies in metres (red = top 3 energy producing nodes, yellow = lowest energy producing node) representing 35 low-level circulation types for the Eastern Cape (20° to 30°E; −30° to −35°S)

To explore in more detail (Fig. 8) the seasonality of energy production in the Eastern Cape, the monthly energy production per node is shown (January to February, JFM, row 1; April to June, AMJ, row 2; June to September, JAS, row 3, October to December, OND, row 4). From this analysis, the three nodes with the highest energy potential contribute most to annual production during the winter months (June to August). This is not surprising, given that these nodes are associated with the passage of cold fronts over the Eastern Cape that occur in association with steep pressure gradients caused by the Atlantic Ocean High (Figs. 6 and 7).

Figure 9 shows the average wind speed direction per trained SOM node (averaged across the Eastern Cape domain). Consistent with the wind rose calculated for each of the sites (Fig. 3), the analysis shows the importance of predominantly westerly and easterly wind components for wind energy production in the Eastern Cape. The nodes associated with the highest energy production (marked in red, nodes 8, 15, and 1) have wind directions of ~ 225°, consistent with the marked pressure gradients when the Atlantic Ocean High ridges behind a cold front. For all these cases, the Atlantic High's centre is at 30 °S or further to the north (Fig. 11a to c), which is indicative of the importance of northward displaced synoptic-scale circulation patterns for optimal wind energy production in the Eastern Cape.

The annual frequency distribution map of SOM nodes is shown in Fig. 10. The SOM methodology functions in such a way that the distribution of constituting cases per node is relatively uniform across nodes. Figure 10 also indicates the average energy production per day per node which provides a reasonable proxy by which to compare the strength of each node to provide wind energy (again noting high energy producing nodes 1, 8, and 15).

4.4 Highest wind energy production nodes

To gain further qualitative insights into the energy meteorology of the Eastern Cape, we explore the synoptic patterns (Fig. 7) associated with the best and worst energy producing Eastern Cape circulation types (Fig. 6) in more detail in Fig. 11.

The patterns displayed for the top three energy producing circulation types (nodes 8, 15, and 1, Fig. 11a–c), as noted before, are indicative of the Atlantic Ocean High with a centre near 30 °S ridging behind a cold front and an associated mid-latitude cyclone passing to the south of the country. For all three cases, the net result is pronounced southwesterly flow over the Eastern Cape, parallel to the geopotential height contours, and reinforcing the importance of strong

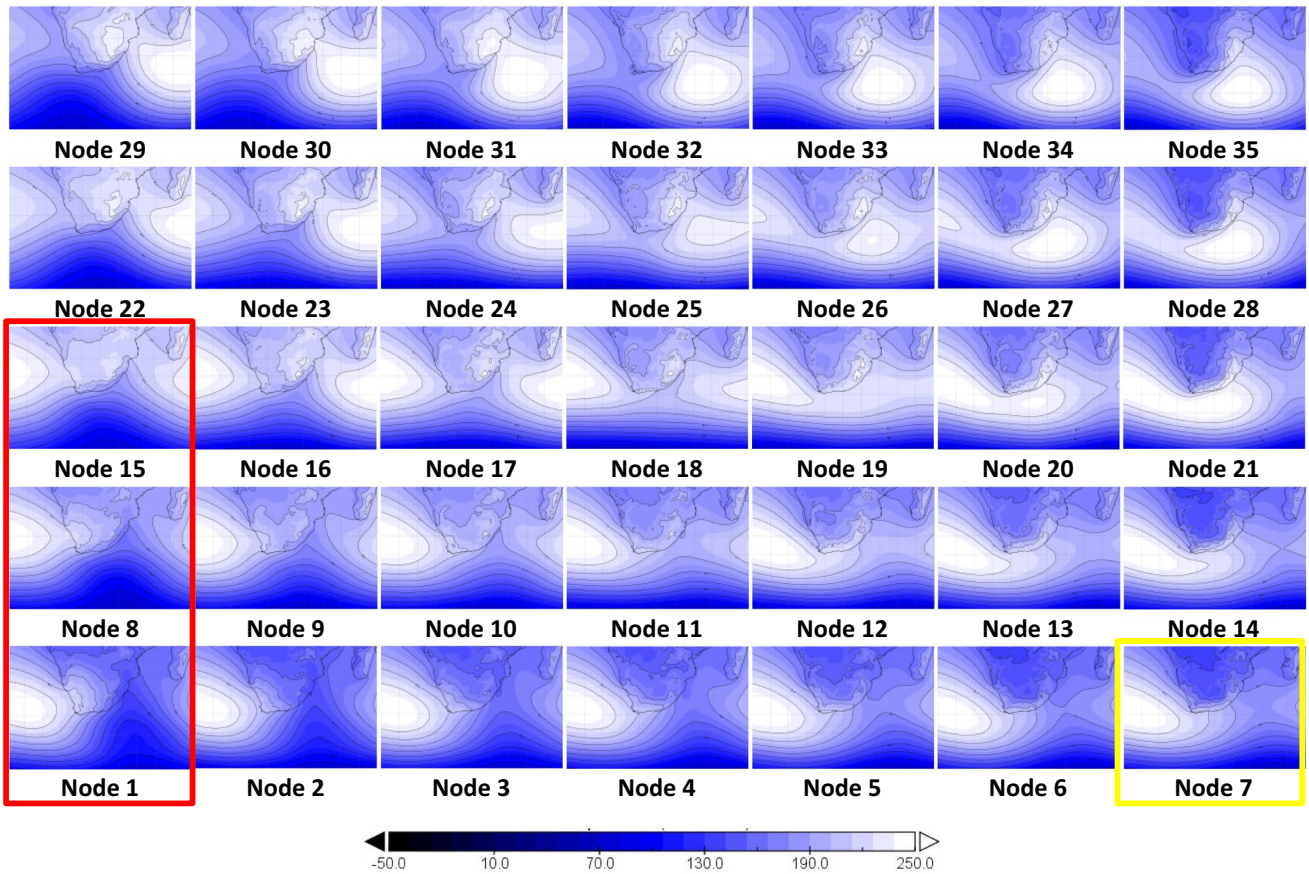

Fig. 7 Accompanying synoptic pattern (geopotential height anomalies in metres) per SOM node (Fig. 6)) (0° to 50°E; −10° to −50°S)

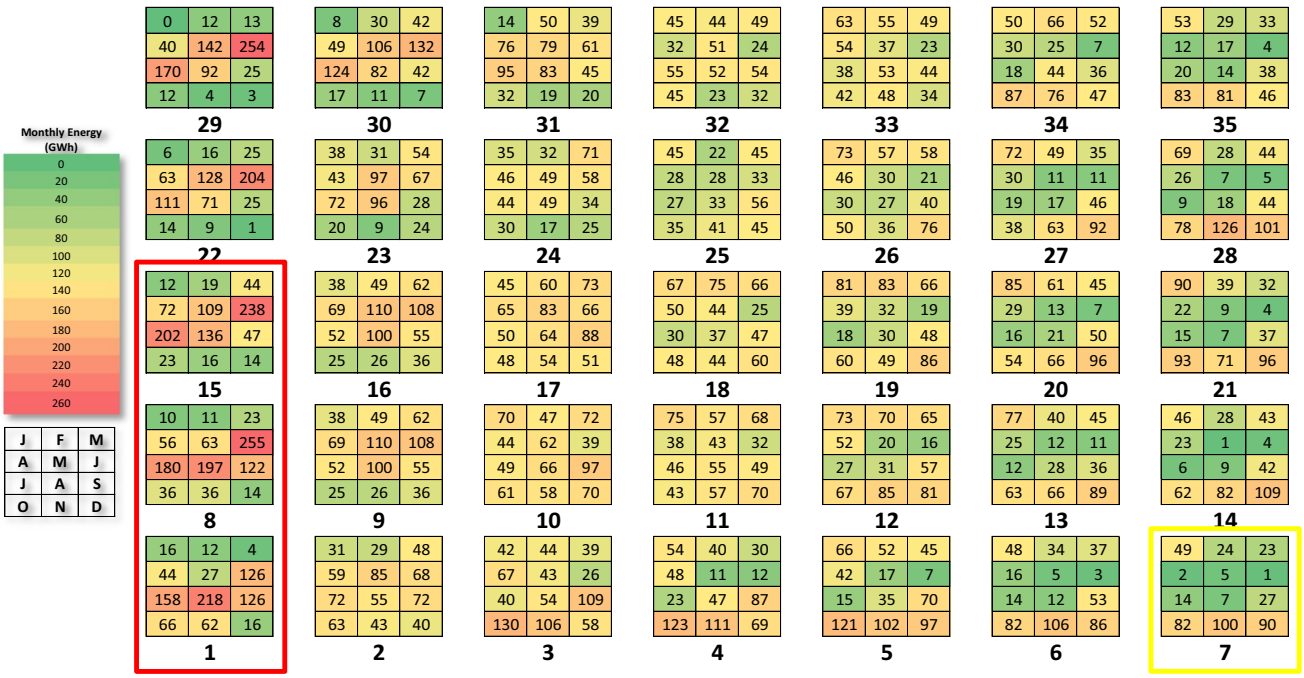

Fig. 8 Monthly total energy distribution per node summed for all four WEF sites (GWh)

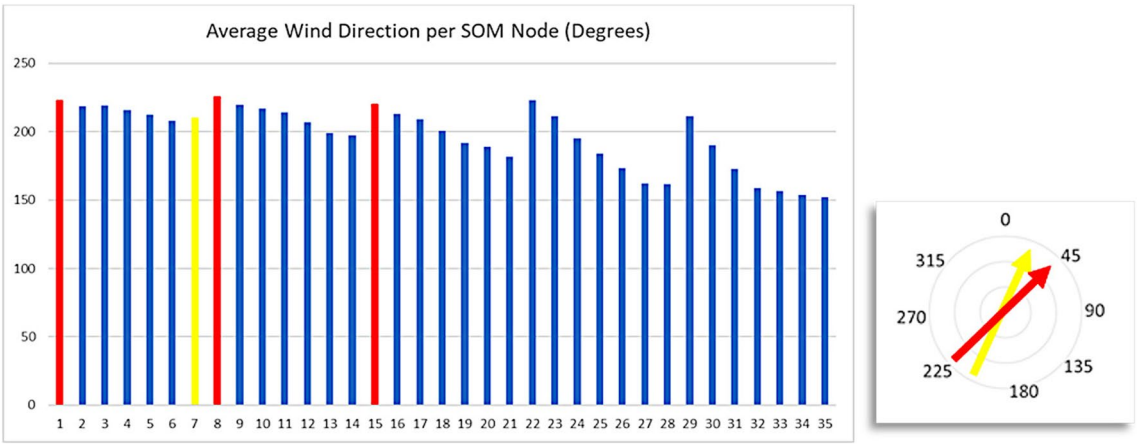

Fig. 9 Average wind direction in degrees from North per trained SOM node

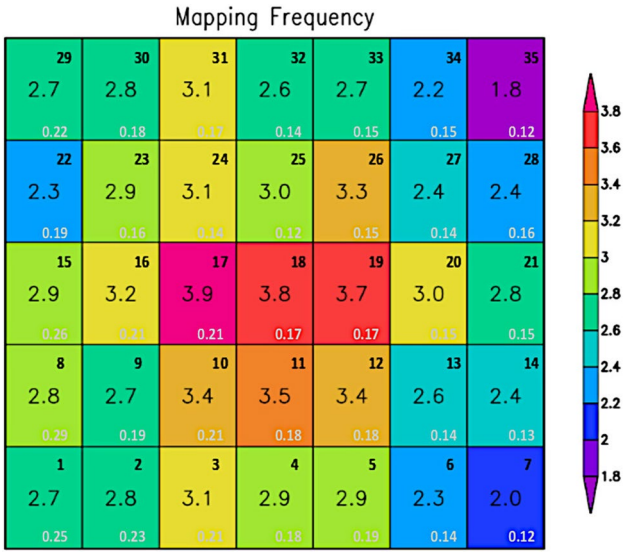

Fig. 10 Trained SOM node annual frequency map (including energy in GWh/day below each frequency), node number in top right corner

southwesterlies for wind energy generation in the Eastern Cape.

A similar study is carried out by Cheneka et al. (2021) and investigates the impact of various weather systems on the Belgian offshore wind fleet energy production using SOMs. In its conclusion, the high wind energy producing SOM nodes display similar characteristics to those identified in this study, i.e. they are characterised by low-pressure systems in front of ridging high-pressure systems similar to the mid-latitude cyclones observed in South Africa (Cheneka et al. 2021).

The circulation type and associated synoptic pattern that has the lowest energy generation potential for the Eastern Cape, node 7 (Fig. 11d), represents mid-latitude cyclones with a more poleward location and a weak ridging high pressure with centre at about 35°S. Pressure gradients are consequently weak over the Eastern Cape, and wind energy production is low.

5 Conclusions

For South Africa to pursue a Just Energy Transition out of its heavy dependence on coal, it needs to increasingly invest in the country's rich resources in wind and solar energy. The Eastern Cape Province has a very high potential for wind energy production and in this research, we explore the relevant energy meteorology and its seasonality in more detail.

The foundation for the study is the long-term meteorological wind mast measurement data available from WASA for four sites in the Eastern Cape, which enabled the calculation of annual and seasonal energy production at four representative locations, in the Eastern Cape. For these energy yield analyses, realistic WEF and WTG designs at each of the four sites are used and run using different software to derive the wind energy production results. The four sites provide good coverage and are representative of the spatial area's energy production potential.

At each of the four sites, annual average wind speeds vary between 7 and 8 m/s, indicating a potentially high wind resource. The energy yield analysis reveals the importance of winter as the season with the highest energy potential. This is not a surprising result, given the northward passage of mid-latitude cyclones over the Southern Ocean in winter. Generally, energy production is the highest around midday and the afternoon, likely because the ocean temperature gradient is then at its steepest, strengthening the pressure gradients and winds.

Following the energy yield analysis, a 35 node SOM was generated to identify the prevailing circulation types of the Eastern Cape, using ERA5 reanalysis data at 6-hourly

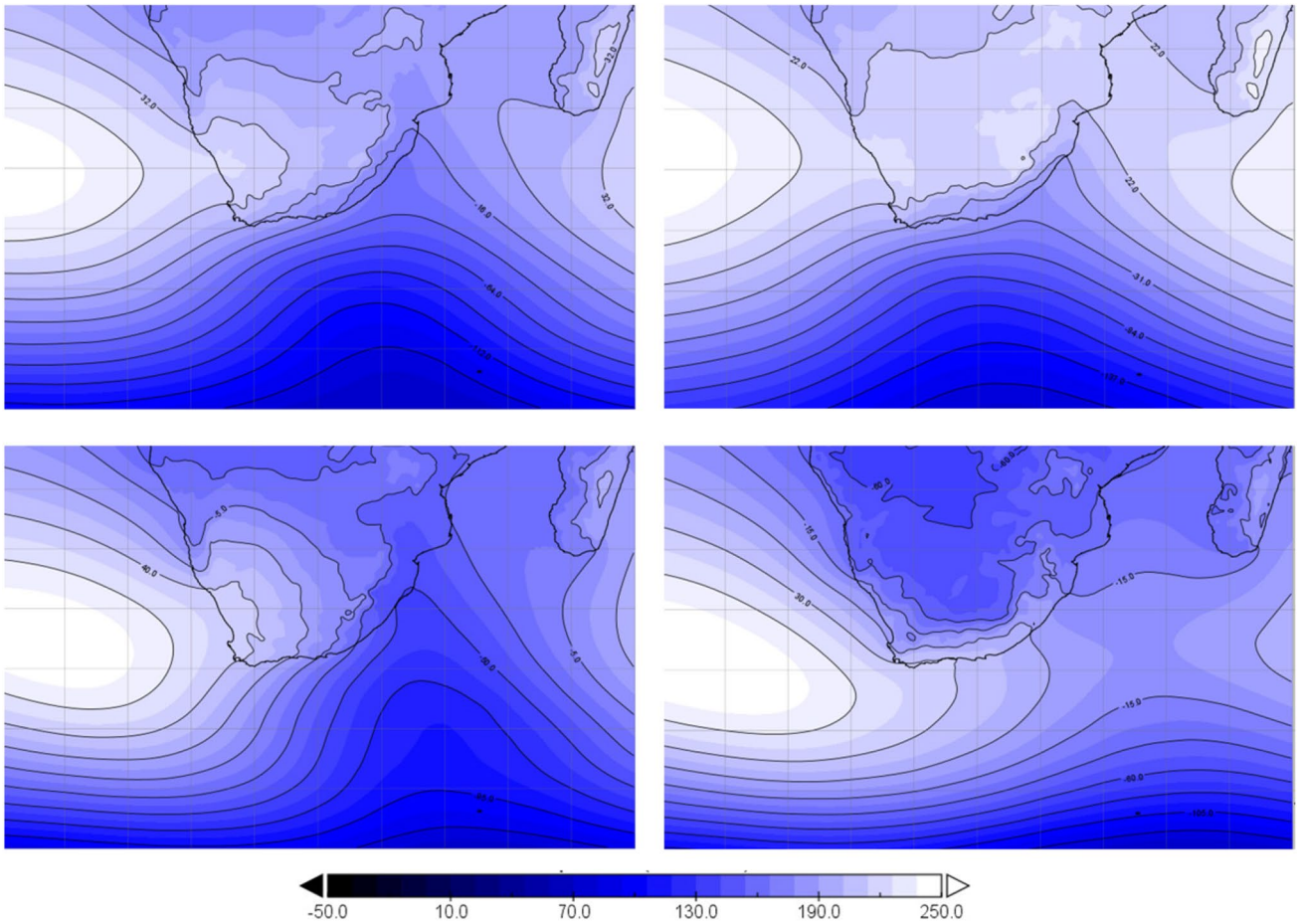

Fig. 11 (**a**) Trained SOM nodes 8, (**b**) 15, (**c**) 1, and (**d**) 7 the greater synoptic pattern 0° to 50°E; −10° to −50°S (geopotential height in metres reduced by spatial average of geographical focus area)

resolution. This SOM result is then mapped onto the 6-hourly P50 energy production. Van Aarde et al. in 2023 follow a similar methodology for South Africa, focusing on resource potential (van Aarde et al. 2023) without taking the next step of providing detailed energy modelling methodologies and results. This study is hereby the first to quantify the energy meteorology of the Eastern Cape, by objectively exploring the detailed P50 energy production of different synoptic types.

The SOM analysis reveals that the synoptic-circulation pattern with the highest energy potential for the Eastern Cape is the Atlantic Ocean ridging high with its centre at about 30 °S, behind a northward displaced mid-latitude cyclone. This results in steep pressure gradients and predominantly south-westerly winds over the Eastern Cape. However, when mid-latitude cyclones pass over the Southern Ocean further to the south, and the Atlantic Ocean High ridges with its centre further to the south at about 35 °S, pressure gradients and energy production are weakest.

SOM nodes 8, 15, and 1 (red outline, Figs. 6, 7, and 8) show the largest potential for energy production. All three of these nodes are characteristic of various stages of a deep mid-latitude cyclone passing to the south of the Eastern Cape, with the Atlantic Ocean High ridging behind the cold front over the Eastern Cape. These three nodes with the highest energy potential contribute most to annual production during the winter months (June to August) and have predominant wind directions of ~ 225°, consistent with the marked pressure gradients when the Atlantic Ocean High ridges behind a cold front.

The methodology developed here, linking energy production at WEF sites to archetypal synoptic types identified by the SOM, provides the foundation for the prediction of wind energy production at various timescales. Particularly, for seasonal forecasts and climate change projections using GCMs whose spatial resolution is relatively low.

This method can be applied to an ensemble of GCMs to project future energy potential through the lens of projected changes in synoptic type frequencies. These changes, in combination with the energy potential associated with the different synoptic types, will effectively yield predictions of future wind energy production. Applications could

include improved understanding of the long-term viability of wind farm sites, guidance on renewable energy development zones, technology selection, and integrated resource planning.

Author contribution All authors contributed to the study conception and design. Material preparation, data collection, and analysis were performed by GL and supported by FE and CL. The first draft of the manuscript was written by GL and all authors commented on previous versions of the manuscript. All authors read and approved the final manuscript.

Funding Open access funding provided by University of the Witwatersrand. This work was supported by the National Research Foundation of South Africa through its Earth System Science Research Programme, Grant 118598.

Data availability The datasets generated during and/or analysed during the current study are available from the corresponding author on reasonable request.

Declarations

Competing interests The authors declare no competing interests.

Open Access This article is licensed under a Creative Commons Attribution 4.0 International License, which permits use, sharing, adaptation, distribution and reproduction in any medium or format, as long as you give appropriate credit to the original author(s) and the source, provide a link to the Creative Commons licence, and indicate if changes were made. The images or other third party material in this article are included in the article's Creative Commons licence, unless indicated otherwise in a credit line to the material. If material is not included in the article's Creative Commons licence and your intended use is not permitted by statutory regulation or exceeds the permitted use, you will need to obtain permission directly from the copyright holder. To view a copy of this licence, visit http://creativecommons.org/licenses/by/4.0/.

References

Charabi Y, Al Hinai A, Al-Yahyai S et al (2019) Offshore wind potential and wind atlas over the Oman Maritime Zone. Energ Ecol Environ 4:1–14. https://doi.org/10.1007/s40974-019-00108-7

Cheneka BR, Watson SJ, Sukanta B (2021) Associating synoptic-scale weather patterns with aggregated offshore wind power production and ramps. Energies 14:3903. https://doi.org/10.3390/en14133903

CSIR Energy Centre (2020) Statistics of utility-scale solar PV, wind and CSP in South Africa. CSIR

Danish Technical University (n.d.-a) WAsP © help files, wind atlas analysis and application program. https://www.wasp.dk/wasp. Accessed June 2020

Danish Technical University (n.d.-b) Wind atlas methodology. https://www.wasp.dk/wasp/wind-atlas-generation/wind-atlas-methodology. Accessed January 2022

Department of Mineral Resources and Energy (n.d.), Renewable independent power producer programme, https://www.gov.za/about-government/government-programmes/renewable-independent-power-producer-programme#, South African Government, accessed October 2023

Department of Mineral Resources and Energy (2003) White paper on renewable energy. South African Government

Department of Mineral Resources and Energy (2019) South Africa integrated resource plan. South African Government

Department of Mineral Resources and Energy (2022) REIPPPP request for proposals, bid window 6, part A: general requirements, rules and provisions, clause 8.3.5. South African Government

Doan QV, Kusaka H, Sato T, Chen F (2020) A structural self-organizing map (S-SOM) algorithm for weather typing. https://doi.org/10.5194/gmd-2020-278

Engelbrecht F, Steinkopf J (2022) Verification of ERA5 and ERA-Interim precipitation over Africa at intra-annual and interannual timescales. Atmos Res 280:106427. https://doi.org/10.1016/j.atmosres.2022.106427

Engelbrecht, C., Landman, W., Engelbrecht, F., & Malherbe, J., A synoptic decomposition of rainfall over the Cape south coast of South Africa, Climate Dynamics Observational, Theoretical and Computational Research on the Climate System, ISSN 0930-7575, Volume 44, Combined 9-10, 2014

Engelbrecht CJ, Engelbrecht FA, Dyson LL (2013) High-resolution model-projected changes in mid-tropospheric closed-lows and extreme rainfall events over southern Africa. Int J Climatol 33(173-187):2012. https://doi.org/10.1002/joc.3420

Engelbrecht F, Adegoke J, Bopape MM, Naidoo M, Garland R, Thatcher M, McGregor J, Katzfey J, Werner M, Ichoku C, Gatebe C (2015) Projections of rapidly rising surface temperatures over Africa under low mitigation. Environ Res Lett 10(8):085004. https://doi.org/10.1088/1748-9326/10/8/085004

Eskom Holdings (n.d.), https://www.eskom.co.za/about-eskom/company-information/, accessed Feb 2023

Eskom Holdings (2022) Generation connection capacity assessment of the 2022 transmission network (GCCA). Eskom Holdings

European Centre for Medium-Range Weather Forecasts, ERA5 (n.d.), https://www.ecmwf.int/en/forecasts/datasets/reanalysis-datasets/era5, accessed May 2021

European Commission (2022) Joint statement: South Africa just energy transition investment plan. https://ec.europa.eu/commission/presscorner/detail/en/statement_22_6664. Accessed November 2023

Frew B et al (2017) 8760-based method for representing variable generation capacity value in capacity expansion models. National Renewable Energy Laboratory

Gruber K, Regner P, Wehrle S, Zeyringer M, Schmidt J (2022) Towards global validation of wind power simulations: a multi-country assessment of wind power simulation from MERRA-2 and ERA-5 reanalyses bias-corrected with the global wind atlas. Energy 238(Part A):121520, ISSN 0360-5442. https://doi.org/10.1016/j.energy.2021.121520

Hahmann AN, Sīle T, Witha B, Davis NN, Dörenkämper M, Ezber Y, García-Bustamante E, González-Rouco JF, Navarro J, Olsen BT, Söderberg S (2020) The making of the New European Wind Atlas – part 1: model sensitivity. Geosci Model Dev 13:5053–5078. https://doi.org/10.5194/gmd-13-5053-2020

Hersbach H et al (2020) The ERA5 global reanalysis, quarterly journal of the royal meteorological society. John Wiley & Sons Ltd on behalf of the Royal Meteorological Society

Hewitson BC, Crane RG (2002) Self organizing maps: applications to synoptic climatology. Clim Res 22:13–26

Hope PK (2006) Projected future changes in synoptic systems influencing southwest Western Australia. Clim Dyn 26:765–780

IEA (2022) World energy outlook 2022. IEA, Paris. https://www.iea.org/reports/world-energy-outlook-2022

Khan T, Theppaya T, Taweekun J (2023) Wind resource assessment of northern part of Thailand. Ain Shams Eng J 14(7):102025, ISSN 2090-4479,. https://doi.org/10.1016/j.asej.2022.102025

Kohonen T, Hynninen J, Kangas J, Laaksonen J (1996) SOMPAK: the self organizing map program package. Helsinki University of Technology, Report A31,

Lennard C, Hegerl G (2014) Relating changes in synoptic circulation to the surface rainfall response using self-organising maps. Clim Dyn:1–19. https://doi.org/10.1007/s00382-014-2169-6

Nassar Y, El-Khozondar HJ, Ghaboun G, Khaleel M, Yusupov Z, Ahmed AA, Alsharif A (2023) Solar and wind atlas for Libya. Int J Electr Eng Sustain (IJEES) 1(3):27–43 Retrieved from https://ijees.org/index.php/ijees/article/view/44

Ndarana T., Mpati S., Bopape M.-J. and Engelbrecht F. (2020). The flow and moisture fluxes associated with ridging South Atlantic Ocean anticyclones during the subtropical southern African summer. Int J Climatol 41 E1000-E1017. https://doi.org/10.1002/joc.6745, July 2020.

Pinto I, Lennard C, Tadross M, Hewitson B, Dosio A, Nikulin G, Panitz H-J, Shongwe ME (2015) Evaluation and projections of extreme precipitation over Southern Africa from two CORDEX models. Clim Change. https://doi.org/10.1007/s10584-015-1573-1

Sammon JW (1969) A nonlinear mapping for data structure analysis. IEEE Trans Comput C18:401–409

Sheridan S, Lee C (2011) The self-organizing map in synoptic climatological research. Kent State University, USA

South African census 2011, https://www.statssa.gov.za/publications/P03014/P030142011.pdf, Statistics South Africa, accessed Nov 2021

The wind atlas of South Africa (n.d.), http://www.wasaproject.info/, CSIR, accessed November 2019

Tyson P (1964) Berg winds of South Africa. Weather 19(1):7–11

Tyson P, Preston-Whyte R (1988) The weather and climate of Southern Africa, 2nd edn, first published. Oxford University Press

Underwriter Labs (n.d.), Openwind user manual, https://openwind.ul-renewables.com/basicwakemodels.html?q=modified+park, accessed Jan 2023

Underwriter Labs (UL) (2010) Openwind theoretical basis and validation. AWS Truepower

van Aarde P, Dalton A, Bekker B (2023) Analysing the relationship between weather systems and wind resource potential and variability in South Africa. In: 58th International Universities Power Engineering Conference (UPEC), vol 2023, Dublin, Ireland, pp 1–6. https://doi.org/10.1109/UPEC57427.2023.10294555

Publisher's note Springer Nature remains neutral with regard to jurisdictional claims in published maps and institutional affiliations.